


# Decrypting the boiling crisis through data-driven exploration of high-resolution infrared thermometry measurements


Cite as: Appl. Phys. Lett. **118**, 253903 (2021); <https://doi.org/10.1063/5.0048391>

Submitted: 22 February 2021 • Accepted: 27 May 2021 • Published Online: 23 June 2021

Madhumitha Ravichandran, Guanyu Su, Chi Wang, et al.

## COLLECTIONS

 This paper was selected as Featured

 This paper was selected as Scilight



View Online



Export Citation



CrossMark

## ARTICLES YOU MAY BE INTERESTED IN

[The not-so-subtle flaws of the force balance approach to predict the departure of bubbles in boiling heat transfer](#)

Physics of Fluids **33**, 017110 (2021); <https://doi.org/10.1063/5.0036956>

[Structured surfaces for enhanced pool boiling heat transfer](#)

Applied Physics Letters **100**, 241603 (2012); <https://doi.org/10.1063/1.4724190>

[Machine learning enables new approach to solve the boiling crisis](#)

Scilight **2021**, 261104 (2021); <https://doi.org/10.1063/10.0005529>

Lock-in Amplifiers  
up to 600 MHz



Zurich  
Instruments



# Decrypting the boiling crisis through data-driven exploration of high-resolution infrared thermometry measurements



Cite as: Appl. Phys. Lett. **118**, 253903 (2021); doi: 10.1063/5.0048391

Submitted: 22 February 2021 · Accepted: 27 May 2021 ·

Published Online: 23 June 2021



View Online



Export Citation



CrossMark

Madhumitha Ravichandran,<sup>1</sup> Guanyu Su,<sup>1</sup> Chi Wang,<sup>1</sup> Jee Hyun Seong,<sup>1</sup> Artyom Kossolapov,<sup>1</sup>  Bren Phillips,<sup>1</sup> Md Mahamudur Rahman,<sup>1,2</sup> and Matteo Bucci<sup>1,a)</sup> 

## AFFILIATIONS

<sup>1</sup>Department of Nuclear Science and Engineering, Massachusetts Institute of Technology, Cambridge, Massachusetts 02139, USA

<sup>2</sup>Department of Mechanical Engineering, University of Texas at El Paso, El Paso, Texas 79968, USA

<sup>a)</sup>Author to whom correspondence should be addressed: [mbucci@mit.edu](mailto:mbucci@mit.edu)

## ABSTRACT

We develop a neural network model capable of predicting the margin to the boiling crisis (i.e., the departure from nucleate boiling ratio, DNBR) from high-resolution infrared measurements of the bubble dynamics on surfaces with different morphologies and wettability (or wickability). We use a feature ranking algorithm, i.e., minimum redundancy maximum relevance, to elucidate the importance of fundamental boiling parameters, i.e., nucleation site density, bubble departure frequency, growth time, and footprint radius, in predicting the boiling crisis. We conclude that these parameters are all necessary and equally important. This result has profound implications, as it undermines the general validity of many observations and mechanistic models that attempt to predict the critical heat flux (CHF) by describing how a single boiling parameter changes with the heat flux or from one surface to another. Notably, the neural network model can predict the DNBR on CHF-enhancing surfaces of different wickability without using any input information related to the surface properties. This result suggests that, at least on the considered surfaces, surface wickability enhances the CHF by modifying the bubble dynamics, i.e., the aforesaid boiling parameters, rather than acting as an additional heat removal mechanism.

© 2021 Author(s). All article content, except where otherwise noted, is licensed under a Creative Commons Attribution (CC BY) license (<http://creativecommons.org/licenses/by/4.0/>). <https://doi.org/10.1063/5.0048391>

Boiling heat transfer is an exceptionally effective heat removal process used for thermal management in many engineering systems, as diverse as nuclear reactors and computer processing units. However, a boiling crisis occurs if the heat flux to remove is too high. When the heat flux exceeds the so-called critical heat flux (CHF), the temperature of the heating surface may rapidly rise above the system design limit, burn out the heat transfer surface, and damage the system irreparably. This runaway temperature escalation is due to the formation of a stable vapor layer with poor heat transfer properties, which isolates the heating surface from the liquid.

The mechanism that triggers the formation of this stable vapor layer, i.e., the boiling crisis, is rather controversial. There is a long-standing debate on whether the boiling crisis is the consequence of far-field hydrodynamic instabilities<sup>1</sup> or a near-wall phenomenon.<sup>2</sup> Also, while it is widely recognized that surface properties affect the CHF limit, the debate on the mechanisms that lead to the enhancement of CHF on wicking surfaces, i.e., porous and hydrophilic surfaces that wick liquids, is particularly vibrant.

Some authors have attributed CHF enhancements to the increase in roughness and, consequently, surface wettability.<sup>3</sup> This idea leverages Kandlikar's CHF model,<sup>4</sup> which was one of the first to consider the effect of wettability on CHF. Other scientists have correlated the CHF enhancements with how fast these surfaces wick liquids. Precisely, some authors have suggested that the CHF enhancement is enabled by an additional heat removal mechanism, i.e., the evaporation of the wicked liquid at the bubble base.<sup>5–7</sup> Instead, Dhillon *et al.* have proposed that the wicking of liquid at the bubble base increases CHF by decreasing the bubble growth time (i.e., by facilitating the departure of bubbles) and consequently decreasing the rise of surface temperature at the bubble base during its growth.<sup>8</sup> Interestingly, Zou and Maroo have reported that even non-wicking micro-structures (e.g., ridges) can increase CHF by decreasing the bubble growth time and increasing the bubble departure frequency.<sup>9</sup> Here, the decrease in growth time was attributed to the rapid evaporation of the liquid trapped within the structures and the increase in CHF to the larger amount of energy transferred through the bubble life cycle per unit

time. A similar idea was explored by Raghupathi and Kandlikar, who discussed how to enhance CHF by increasing the contact line density.<sup>10</sup>

Machine learning offers the possibility to investigate this phenomenon, which does not have, to date, a clear, definitive mathematical description, with a fresh, hypothesis-free approach. However, the use of these techniques to analyze boiling experiments is still in its infancy, and so far, has been limited to diagnostic and prognostic purposes.<sup>11–14</sup>

In this work, we use machine learning algorithms to explore the connection between fundamental boiling parameters (e.g., nucleation site density, bubble departure frequency, growth time, and footprint radius) and the boiling crisis by analyzing high-resolution infrared measurements of the boiling process. Precisely, we combine high-resolution infrared measurements and neural networks to predict the departure from nucleate boiling ratio, DNBR, defined as

$$\text{DNBR} = \frac{q''_{\text{CHF}}}{q''}, \quad (1)$$

without knowing the imposed heat flux,  $q''$ , or the actual critical heat flux,  $q''_{\text{CHF}}$ . Also, we use feature ranking algorithms to elucidate the importance of the aforementioned boiling parameters in making accurate predictions.

We perform pool boiling investigations featuring high-speed infrared (IR) thermometry with water at ambient pressure on surfaces with different morphologies and intrinsic wettability. The heaters consist of an IR-transparent sapphire substrate coated with a thin electrically conductive layer, e.g., indium tin oxide (ITO), as sketched in Fig. 1. This layer is in contact with water. It has negligible thermal resistance and heat capacity, and it is perfectly IR opaque. Its surface can be modified to induce changes in intrinsic wettability and wickability. In this paper, we cover the boiling surface with copper oxide (CuO) nanoleaves, zinc oxide (ZnO) nanowires, and layers of silicon dioxide (SiO<sub>2</sub>) nanoparticles. These three coatings make the surface super-hydrophilic and enhance the CHF compared to the uncoated surface. Details about the characterization of these surfaces and their CHF values can be found in the [supplementary material](#). In a typical experiment, we control the power released by the thin, IR opaque, electrically conductive layer and measure the time- and space-dependent radiation that it emits through the sapphire. Bubble growth and departure induce spatial and temporal changes in the surface temperature and, accordingly, in the IR radiation. Practically, this IR radiation (captured with a temporal resolution of 0.4 ms and a pixel size of 115  $\mu\text{m}$ , in this paper) can be post-processed to measure the time-dependent temperature and heat flux distributions on the boiling surface.<sup>15</sup> Based on these distributions, we can identify the position and the number of the nucleation sites and measure the bubble growth time, wait time, and footprint area.<sup>16</sup>

We develop an artificial neural network (ANN) model that can evaluate the DNBR directly from the IR radiation (expressed in counts) emitted by the boiling surface. Precisely, the list of ANN input features includes the nucleation site density,  $N''$ , and the statistical moments of the infrared radiation at the nucleation sites, through which we seek to capture the effect of other boiling parameters on the boiling crisis. We consider mean, standard deviation, skewness, and kurtosis of IR counts, their first derivative in space and time, and their second derivative in space. This neural network is trained using

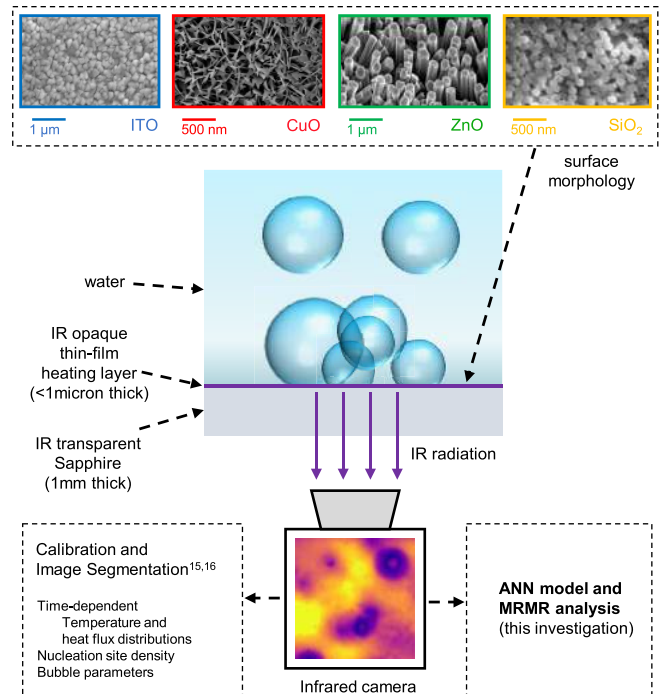


**FIG. 1.** Synopsis of the methodology including saturated pool boiling experiments with water at ambient pressure on surfaces with different morphologies and wettability and featuring high-resolution infrared diagnostics.

experimental data points from only three surfaces (plain ITO, copper oxide nanoleaves, and zinc oxide nanowires). 15% of the total data points from these three surfaces are reserved for testing. Training and validation of the network are carried out using the remaining data points. We use 10-fold cross validation with the standard method of data partitioning. Once network training is complete, we test the network performance on the reserved 15% of the data points from the three surfaces, and all the data for the fourth surface (i.e., the porous layer made of silicon dioxide nanoparticles), which is not used for the training. Details about the preparation of the input features and the neural network architectures, their training and testing, and additional training checks, e.g., to exclude the possibility of memorization or overfitting, can be found in the [supplementary material](#).

The predictions of the trained neural network on both the training and testing data are presented in Fig. 2 (top). We observe that predictions are consistent with the experimentally determined DNBR. No matter the surface, the trained neural network model can determine the DNBR with a mean absolute percentage error complement (i.e., 100–MAPE) of  $\sim 96\%$  even though no direct information on the heat flux or the surface properties, or the physical mechanisms was included in the input features. This result suggests that the ANN is able to map the triggering mechanism of the boiling crisis directly from the data it was trained on. However, while the selected input features are sufficient to determine the DNBR with little error, they may not be all necessary. We use a feature ranking algorithm, i.e., minimum redundancy and maximum relevance<sup>17</sup> (MRMR), to identify the most important ones. The MRMR algorithm consists of determining

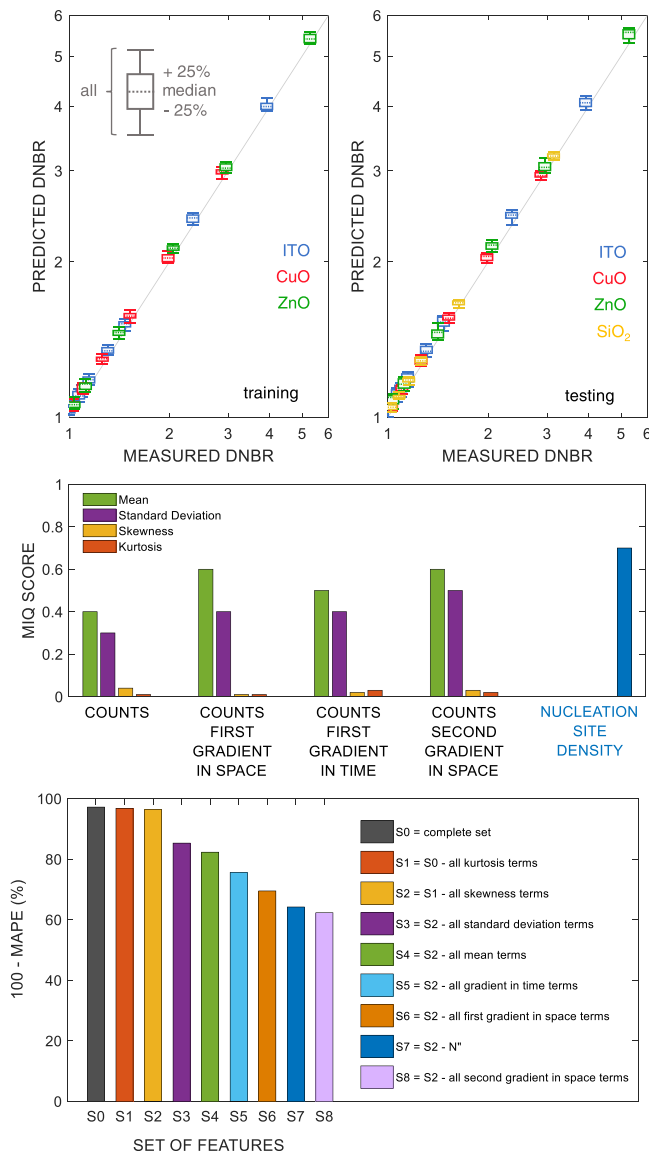


**FIG. 2.** Comparison between predicted and measured DNBR for the complete set of features (top), MRMR analysis (aggregating training and testing data) on the input features used to predict DNBR with the complete set of features (middle) and 100-MAPE (aggregating training and testing data) of the DNBR prediction with reduced sets of features (bottom).

the correlation within the input variables and between input and output variables. The former is a measure of the redundancy of a feature set, whereas the latter quantifies the relevance of a feature set with respect to the output variable. The correlation is mapped through the mutual information,  $I$ . Qualitatively,  $I$  characterizes how much uncertainty of one variable can be reduced by knowing the other variable and vice versa (see the [supplementary material](#) for the mathematical details). Thus, the redundancy,  $D$ , of a feature,  $F_i$ , with respect to the  $n$  features in the input set is given by

$$D(F_i) = \frac{1}{n} \sum_{t=1:n} I(F_i, F_t). \quad (2)$$

Instead, the relevance,  $V$ , of this feature with respect to the output variable,  $T$ , e.g., the DNBR, is given by

$$V(F_i) = I(F_i, T). \quad (3)$$

The ratio of relevance to redundancy gives the mutual information quotient,  $MIQ(F_i)$ , the magnitude of which is used to rank the features

$$MIQ(F_i) = \frac{V(F_i)}{D(F_i)}. \quad (4)$$

A high MIQ value indicates an important feature. Conversely, a null or low value indicates an irrelevant or redundant feature.

The results of the MRMR analysis are shown in [Fig. 2](#) (middle). Briefly, the nucleation site density,  $N''$ , has the maximum MIQ score with the other spatiotemporal parameters also contributing significantly to the prediction. However, the higher-order moments (skewness and kurtosis) have a much lower score and are expected to contribute very little. We corroborate this analysis by developing neural network models with reduced sets of input parameters. [Figure 2](#) (bottom) shows how the performance of the ANN approach changes after eliminating selected input parameters. As shown, eliminating the higher-order moments, i.e., using the set of features S1 and S2, does not affect the prediction. However, eliminating the lower order moments or the nucleation site density (sets S3–S8) degrades the prediction significantly. In summary, all the input features except the higher-order moments (i.e., the set S2) are required to predict the boiling crisis, i.e.,  $DNBR = 1$ .

To explore the causal relationships between the DNBR and the fundamental bubble parameters (i.e., bubble departure frequency, growth time, and footprint radius), we conduct a similar analysis. We start by developing neural networks to predict, from the set of features  $\Omega_0 = S_7$  (i.e., all the DNBR features except the nucleation site density), the bubble footprint radius,  $R$ , and the product of bubble growth time and frequency,  $f t_g$ , which expresses the probability to have a bubble growing at a given nucleation site. The results in [Fig. 3](#) (top, left and right) show that this set of parameters allows predicting these boiling parameters quite well (note that these plots aggregate training and testing data) and motivate the following questions: are all these parameters necessary? and, are  $f t_g$  and  $R$  mutually dependent, i.e., do they share the same minimum set of input features?

To answer these questions, we use the same approach as for the DNBR, i.e., we evaluate the capability to capture these fundamental parameters with reduced sets of input features. Interestingly, the results in [Fig. 3](#) (bottom) reveal that removing the gradient in time from the complete set  $\Omega_0$ , i.e., using the feature set  $\Omega_1$ , does not deteriorate the  $f t_g$  predictions. Instead, the error increases if we remove any of the spatial parameters. Similarly, a slightly different set,  $\Omega_2$ , is necessary and sufficient to predict the average bubble footprint radius with an acceptable error. We see that  $\Omega_1$  is different from  $\Omega_2$ , i.e., it is unlikely that  $f t_g$  and the bubble footprint radius are mutually dependent. However, the union of  $\Omega_1$  and  $\Omega_2$  yields  $\Omega_0$ .  $\Omega_0$  along with the nucleation site density yields S2, i.e., the minimum set of features to predict DNBR. This observation suggests that we could predict the DNBR directly from  $N''$ ,  $f t_g$ , and  $R$ .

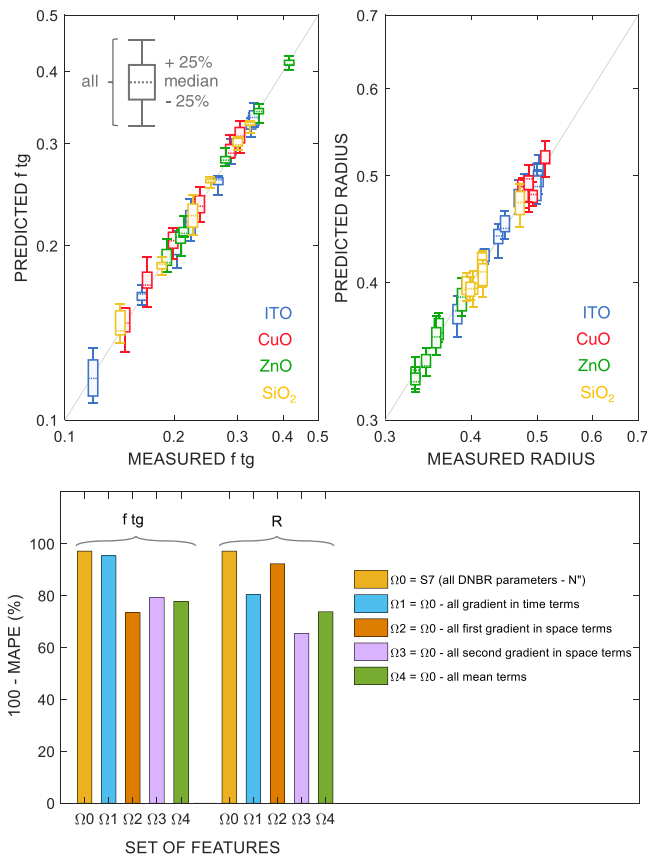


**FIG. 3.** Comparison between the predicted and measured  $f_{tg}$  (top left) and radius (in mm, top right) for the complete set of features, and (bottom) 100-MAPE of these predictions with reduced sets of features.

To explore this hypothesis, we develop ANN models to predict the DNBR using these three boiling parameters as inputs and conduct an MRMR analysis. Figure 4 shows the results of this analysis. All the parameters have non-zero and comparable MIQ, i.e., they are all relevant to predict the DNBR. When one of them is removed from the input features set, the DNBR predictions degrade considerably. These results are also confirmed by a simple low-order regression of the data and, importantly, while the analysis presented in Fig. 4 aggregates all

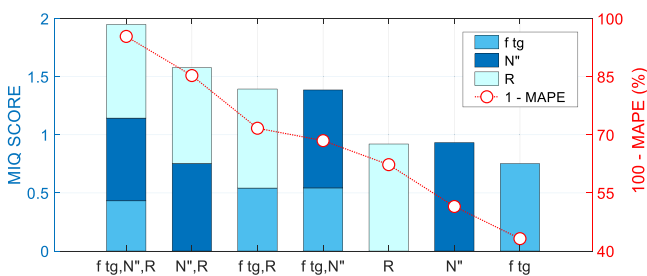


**FIG. 4.** MRMR analysis of the boiling parameters ( $f_{tg}$ ,  $N''$ , and  $R$ ) used to predict DNBR and 100-MAPE of the predictions for several combinations of these parameters (secondary y axis).

the surfaces, we found equivalent results when analyzing each surface separately (see the supplementary material). These observations suggest that it is unlikely to have a generalizable boiling crisis model by using mechanistic descriptions that seek to predict the boiling crisis as the outcome of a single effect, e.g., an increase in nucleation site density or a decrease in bubble growth time. Instead, it is essential to combine these three parameters and describe their mutual interaction. Such conclusion seems to corroborate approaches picturing the boiling crisis as a limit of the wall heat flux partitioning,<sup>18</sup> or a recent theory from our group, suggesting that the boiling crisis is due to an instability of the bubble interaction process on the boiling surface, described as a continuum percolation phenomenon.<sup>19,20</sup>

It is noteworthy that, while we have tested the boiling performance of surfaces with different morphologies, wickability, and critical heat flux, our set of input features does not contain any information about these quantities, e.g., we do not use the Wicking number, which is usually considered a first-order indicator of the critical heat flux enhancement on porous and hydrophilic surfaces.<sup>6</sup> Our work suggests that, while wickability certainly enhances CHF, the mechanism may not be related to the evaporation of the wicked liquid but to how these surfaces change bubble departure frequency, growth time, footprint radius, and nucleation site density. Also, note that all this analysis implicitly assumes and corroborates the hypothesis that the boiling crisis is a near-wall phenomenon, as we only used information related to the dynamic of bubbles at the heating surface, provided by the infrared thermometry measurements.

In conclusion, we have developed a data-driven methodology to predict the boiling crisis. This methodology consists of artificial neural networks and MRMR feature ranking algorithms and uses the unprocessed time-dependent infrared radiation distributions emitted by the boiling surface as inputs. Based on our analyses, we conclude that generalizable predictions of the DNBR, and consequently the boiling crisis, cannot be obtained by considering a single boiling parameter, but they are possible when based on nucleation site density, bubble footprint radius, and product of bubble frequency and growth time together. This conclusion is supported by the comparison with experimental results obtained on surfaces with different surface properties, e.g., wickability and CHF limits. Finally, based on un-processed, time-dependent infrared radiation distributions, the methodology we developed opens the possibility to monitor the DNBR and estimate the CHF online and in quasi-real-time when conducting boiling experiments using infrared thermometry, which is key toward the implementation of smart, autonomous experiments.

See the supplementary material for the details on the experiment, the implementation of the ANN models, their training and additional checks, the MRMR analysis, the low-order regression model, additional feature ranking analyses conducted using other techniques, and additional results.

We thank Professor J. Buongiorno and Professor E. Baglietto for the enlightening discussions. We acknowledge the support of the Consortium for Advanced Simulations of Light Water Reactors (<http://www.casl.org>), under U.S. Department of Energy Contract No. DEAC05-00OR22725 and the support of the National Science Foundation under Award No. 2019245. M. Ravichandran acknowledges the funding supports of the Schlumberger

Foundation Faculty for The Future (FFTF) and the MIT School of Engineering MathWorks fellowship.

#### DATA AVAILABILITY

The data that support the findings of this study are available from the corresponding author upon reasonable request.

#### REFERENCES

- <sup>1</sup>Z. Novak, "Hydrodynamic aspects of boiling heat transfer," Ph. D. thesis (University of California, Los Angeles, California, 1959).
- <sup>2</sup>T. G. Theofanous and T. N. Dinh, "High heat flux boiling and burnout as microphysical phenomena: Mounting evidence and opportunities," *Multiphase Sci. Technol.* **18**(3), 251 (2006).
- <sup>3</sup>K. H. Chu, Y. Soo Joung, R. Enright, C. R. Buie, and E. N. Wang, "Hierarchically structured surfaces for boiling critical heat flux enhancement," *Appl. Phys. Lett.* **102**(15), 151602 (2013).
- <sup>4</sup>S. G. Kandlikar, "A theoretical model to predict pool boiling CHF incorporating effects of contact angle and orientation," *J. Heat Transfer* **123**(6), 1071–1079 (2001).
- <sup>5</sup>H. D. Kim and M. H. Kim, "Effect of nanoparticle deposition on capillary wicking that influences the critical heat flux in nanofluids," *Appl. Phys. Lett.* **91**(1), 014104 (2007).
- <sup>6</sup>M. M. Rahman, E. Olceroglu, and M. McCarthy, "Role of wickability on the critical heat flux of structured superhydrophilic surfaces," *Langmuir* **30**(37), 11225–11234 (2014).
- <sup>7</sup>M. Tetreault-Friend, R. Azizian, M. Bucci, T. McKrell, J. Buongiorno, M. Rubner, and R. Cohen, "Critical heat flux maxima resulting from the controlled morphology of nanoporous hydrophilic surface layers," *Appl. Phys. Lett.* **108**(24), 243102 (2016).
- <sup>8</sup>N. S. Dhillon, J. Buongiorno, and K. K. Varanasi, "Critical heat flux maxima during boiling crisis on textured surfaces," *Nat. Commun.* **6**(1), 8247 (2015).
- <sup>9</sup>A. Zou and S. C. Maroo, "Critical height of micro/nano structures for pool boiling heat transfer enhancement," *Appl. Phys. Lett.* **103**(22), 221602 (2013).
- <sup>10</sup>P. A. Raghupathi and S. G. Kandlikar, "Pool boiling enhancement through contact line augmentation," *Appl. Phys. Lett.* **110**(20), 204101 (2017).
- <sup>11</sup>G. M. Hobold and A. K. da Silva, "Automatic detection of the onset of film boiling using convolutional neural networks and Bayesian statistics," *Int. J. Heat Mass Transfer* **134**, 262–270 (2019).
- <sup>12</sup>G. M. Hobold and A. K. da Silva, "Visualization-based nucleate boiling heat flux quantification using machine learning," *Int. J. Heat Mass Transfer* **134**, 511–520 (2019).
- <sup>13</sup>G. M. Hobold and A. K. da Silva, "Machine learning classification of boiling regimes with low speed, direct and indirect visualization," *Int. J. Heat Mass Transfer* **125**, 1296–1309 (2018).
- <sup>14</sup>M. Ravichandran and M. Bucci, "Online, quasi-real-time analysis of high-resolution, infrared, boiling heat transfer investigations using artificial neural networks," *Appl. Therm. Eng.* **163**, 114357 (2019).
- <sup>15</sup>M. Bucci, A. Richenderfer, G. Y. Su, T. McKrell, and J. Buongiorno, "A mechanistic IR calibration technique for boiling heat transfer investigations," *Int. J. Multiphase Flow* **83**, 115–127 (2016).
- <sup>16</sup>A. Richenderfer, A. Kossolapov, J. H. Seong, G. Saccone, E. Demarly, R. Kommajosyula, E. Baglietto, J. Buongiorno, and M. Bucci, "Investigation of subcooled flow boiling and CHF using high-resolution diagnostics," *Exp. Therm. Fluid Sci.* **99**, 35–58 (2018).
- <sup>17</sup>C. Ding and H. Peng, "Minimum redundancy feature selection from microarray gene expression data," *J. Bioinf. Comput. Biol.* **03**(2), 185–205 (2005).
- <sup>18</sup>E. Baglietto, E. Demarly, and R. Kommajosyula, "Boiling crisis as the stability limit to wall heat partitioning," *Appl. Phys. Lett.* **114**(10), 103701 (2019).
- <sup>19</sup>L. Zhang, J. H. Seong, and M. Bucci, "Percolative scale-free behavior in the boiling crisis," *Phys. Rev. Lett.* **122**(13), 134501 (2019).
- <sup>20</sup>G. Y. Su, C. Wang, L. Zhang, J. H. Seong, R. Kommajosyula, B. Phillips, and M. Bucci, "Investigation of flow boiling heat transfer and boiling crisis on a rough surface using infrared thermometry," *Int. J. Heat Mass Transfer* **160**, 120134 (2020).